REYNOLDS NUMBER DEPENDENCE OF MATERIAL LINE AND SURFACE STRETCHING IN TURBULENCE

Susumu Goto and Shigeo Kida
Department of Mechanical Engineering, Kyoto University,
Yoshida-Honmachi, Sakyo, Kyoto 606-8501, Japan
susumu-goto@mail-box.jp, kida@mech.kyoto-u.ac.jp

ABSTRACT

It is numerically shown that the stretching rate, normalised by the reciprocal of Kolmogorov time, of long material lines (or wide surfaces) in stationary homogeneous turbulence depends on the Reynolds number. This is contradicting the conventional belief that the material object stretching is solely determined by the smallest-scale eddies. A physical explanation based on the intensive folding of the material objects is suggested to understand the observed Reynolds number dependence of material object stretching.

INTRODUCTION

A material object is defined by the one which always consists of the same set of fluid particles (Batchelor 1952). By this definition, a material line in two-dimensional (2D) space (or a material surface in 3D) is the boundary between two parts of fluid. The deformation of material line (or surface) is, therefore, closely related to the mixing of these two parts (see figures 2 and 3), and their intensive (more precisely, exponential) stretching in turbulence is a manifestation of the strong mixing. Since the turbulence mixing is one of the hottest unresolved problems in this field of research, we desire to understand the mechanism and statistics of material object stretching in turbulence.

It is G.K. Batchelor (1952) who first shed light on the deformations of material lines and surfaces in statistically stationary homogeneous turbulence. He suggested that the material lines (or surfaces) could be regarded as a set of statistically equivalent infinitesimal material line (or surface) elements in stationary homogeneous turbulence, and predicted that the total length $L(t)$ of a material line (or the total area $A(t)$ of a surface) grows exponentially, and that its stretching rate

$$\gamma \equiv \frac{\mathrm{d}}{\mathrm{d}t} \log L \qquad \left(\text{or} \quad \gamma \equiv \frac{\mathrm{d}}{\mathrm{d}t} \log A\right) \tag{1}$$

is independent of the Reynolds number if it is normalised by the reciprocal of Kolmogorov time

$$\tau_\eta \equiv \epsilon^{-\frac{1}{2}}\, \nu^{\frac{1}{2}} \sim \omega'^{-1}\,. \tag{2}$$

Here, ϵ, ν and ω' are the energy dissipation rate per unit mass, the kinematic viscosity of fluid and r.m.s. value of the vorticity.

It has been pointed out (Kida and Goto 2002, Goto and Kida 2002), however, that, in contrast with Batchelor's suggestion, the statistics of finite-sized material objects are different from those of infinitesimal elements because of the fact that the material objects are stretched inhomogeneously by coherent eddies even in homogeneous turbulence, and that we

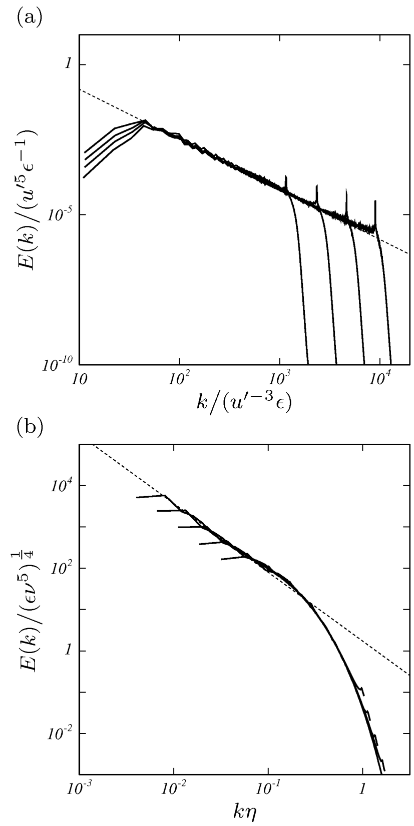

Figure 1: Numerically simulated energy spectra in (a) 2D stationary homogeneous turbulence (inverse energy cascade regime) and (b) 3D stationary homogeneous turbulence. We have simulated four different Reynolds numbers in 2D, and five different Reynolds numbers in 3D. Dashed lines indicate the $k^{-\frac{5}{3}}$ power law.

need to track finite-sized material objects to accurately estimate their statistics by numerical simulations. Recent direct numerical simulation (DNS) of finite-sized material objects shows that material objects are stretched by clusters of coherent eddies at Kolmogorov length scales (Goto and Kida 2003); see also figure 4. One might speculate that material object deformation by (clusters of) these Kolmogorov-scale eddies leads to the Kolmogorov-scaling of stretching rate. In contrast with this conventional idea, however, we have found that the stretching rates cannot be scaled by $\tau_\eta{}^{-1}$ (figure 5).

The purpose of the present article is to resolve this surprising finding in terms of the rapid folding of material objects.

DIRECT NUMERICAL SIMULATION

Numerical scheme

We have performed the DNS of material objects advected by stationary homogeneous isotropic turbulence of an incompressible fluid. Velocity field is governed by the Navier-Stokes equation with an external forcing at large scales in the case of 3D (or at small scales in 2D) and the equation of continuity under periodic boundary conditions. A drag force is also employed in the 2D case in order to avoid the energy accumulation at large scales. The energy spectra, in both cases of 3D and 2D, are proportional to $k^{-5/3}$ in the inertial range because of the forward (in 3D) or the backward (in 2D) energy cascade (figure 1). We have simulated five different Taylor-length based Reynolds numbers, $R_\lambda = \sqrt{\frac{30}{2\nu\epsilon}}\, u'^2$ ranging between 57 and 252 in 3D by using grid points up to 512^3. Here, u' is the r.m.s. value of a velocity component. As seen in figure 1(b), it is not still fully developed; that is, the ratio of the integral scale $\mathcal{L}$ to the Kolmogorov scale $\eta\,(\equiv \epsilon^{-\frac{1}{4}}\nu^{\frac{3}{4}})$ is $O(10)$. While in the 2D turbulence, we can simulate fully developed turbulence, by employing 4096^2 grids, which reveals the $k^{-\frac{5}{3}}$ power law spectrum over nearly two decades. The details of the numerical schemes and parameters of the present DNS are described in Goto and Kida (2003) for the 3D case and Goto and Vassilicos (2004) for 2D.

In the present DNS, material lines (or surfaces) are expressed by a chain of short line segments (or a set of small triangles), and the temporal evolution of the position vectors of these line segments (or triangles) are tracked by solving the advection equations

$$\frac{\mathrm{d}}{\mathrm{d}t}\,\boldsymbol{x}_p = \boldsymbol{u}(\boldsymbol{x}_p(t), t) \qquad (3)$$

for vertexes $\boldsymbol{x}_p(t)$ of the line segments (or triangles). The right-hand side of (3) is estimated by an interpolation of velocity field $\boldsymbol{u}(\boldsymbol{x}, t)$ at numerical grids. Interpolations are employed at every time step in order to keep the line segments (or the sides of triangles) short enough compared to the Kolmogorov length.

Temporal evolution of stretching rate

The typical temporal evolutions of a material line and a surface are shown in figures 2 and 3, respectively. They seem to be deformed by turbulence in a quite complicated manner. Nevertheless, by plotting the deformed material line in 2D together with the vorticity field in figure 4, we can see the deformation is closely related to the coherent vortical structures at the smallest scales. Note that in this 2D turbulence of the inverse energy cascade regime the vortical structures are dominated at the smallest scale, since the enstrophy spectrum peaks in a high wavenumber region (the energy spectrum is proportional to $k^{-\frac{5}{3}}$ in the inertial rage, as seen in figure 1, and therefore the enstrophy spectrum is proportional to $k^{+\frac{1}{3}}$). This observation implies that the deformation of material objects is governed by the smallest-scale eddies. Similarly to this 2D observation, it has been reported that the Kolmogorov scale eddies play crucial roles in the deformations of material

(a)
(b)
(c)

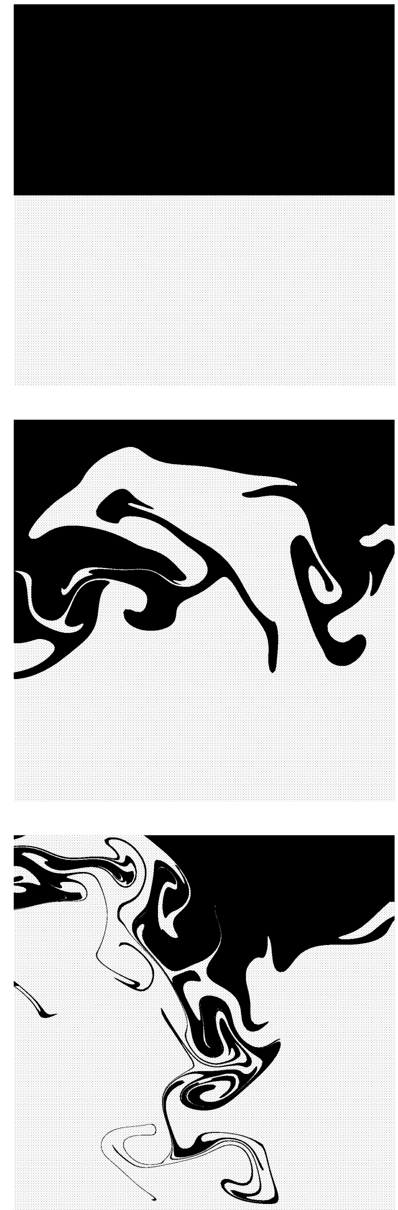

Figure 2: The temporal evolution of a material line, which is the boundary between two coloured regions, in 2D stationary homogeneous turbulence (inverse energy cascade regime). The size of shown box is about 6.5η. (a) $t = 0$, (b) $5\tau_\eta$ and (c) $10\tau_\eta$.

lines in 3D homogeneous turbulence. For example, the average curvature of deformed material lines is $O(10\eta)$ irrespective of the Reynolds number (Goto and Kida 2003).

Therefore, we may expect that the stretching rate (1) is also independent of the Reynolds number if it is normalised by ${\tau_\eta}^{-1}$, which is proportional to the r.m.s value of the vorticity. However, this is not the case as seen in figure 5. We plot in the figure the numerically estimated stretching rates of material lines in 2D and of lines and surfaces in 3D as a function of normalised time. The initial conditions of these material lines (or surfaces) are the straight lines (or flat square surfaces) which

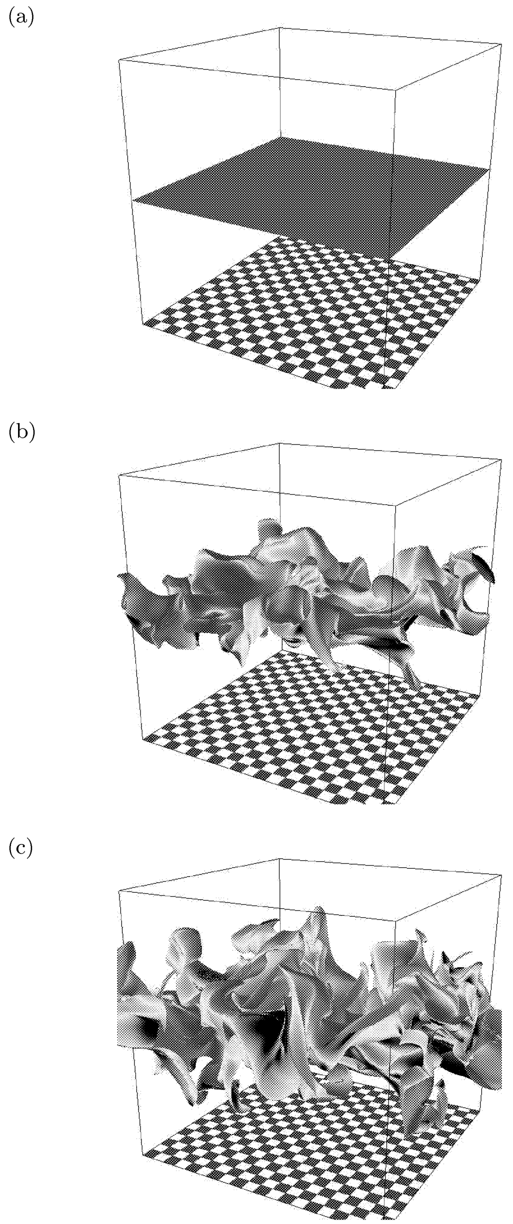

Figure 3: The temporal evolution of a material surface in 3D stationary homogeneous turbulence. Shown box is the periodic box of the velocity field; its side is about 200η. (a) $t = 0$, (b) $5\tau_\eta$ and (c) $10\tau_\eta$.

are sufficiently longer (or wider) than $\mathcal{L}$ (or $\mathcal{L}^2$). Because of the independency between the strain field and the direction of the material objects, the mean stretching rate vanishes initially. After some transient time, the stretching rates clearly depend on the Reynolds number; the higher Reynolds number is, the larger the stretching rates become. Because of the rapid growth of the total length of lines (or area of surfaces) it is not possible to track them for a long time. So it has not been conclusive, but we can conjecture that γ saturates at the later times to different values for different Reynolds numbers (figure 5(a)).

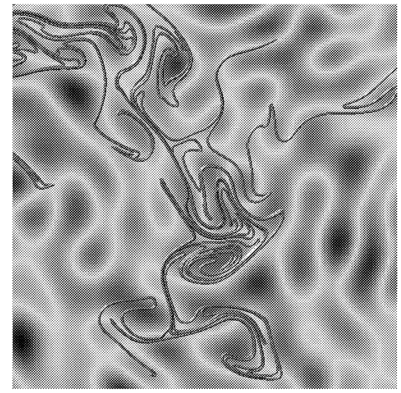

Figure 4: Deformed material line in 2D turbulence (same as figure 2(c)) is plotted together with the magnitude of vorticity.

PHYSICAL EXPLANATION OF THE REYNOLDS NUMBER DEPENDENCE

Rapid folding

The key notion to understand the Reynolds number dependence of material line (or surface) stretching is the intensive folding. As seen in the visualisation of material objects (e.g. figure 2), they are quite intensively folded. This is because while the extent of material line (or surface) grows only algebraically, its total length (or its total area) grows exponentially. On the other hand, because of the incompressibility of fluid, the folded parts of lines (or surfaces) tend to accumulate in large stretching regions. Hence, if the folding is effective, then the average stretching rate gets larger because stronger stretching parts are more weighted by the accumulation by folding.

Recall that the Reynolds number R_λ is proportional to $(\mathcal{L}/\eta)^{\frac{3}{2}}$. Therefore, at a higher Reynolds number, turbulence consists of eddies in wider ranges of length scales. For the stretching of material objects only the smallest-scale eddies, which has the smallest turnover time, are important. However, for their folding, eddies at all length scales play roles. It is, therefore, intuitively clear that the efficiency of folding is different at different Reynolds numbers. This is a reason why the stretching rate of sufficiently long lines (or wide surfaces) depends on the Reynolds number.

Numerical verification

In order to numerically verify the physical explanation that the Reynolds number dependence of stretching rate comes from the folding we have carried out two preliminary numerical tests using material lines in 2D DNS.

The first test is the DNS of infinitesimal lines. The infinitesimal objects cannot be folded, and we expect that the average stretching rate does not depend on the Reynolds number. Indeed, this is the case as seen in figure 6(a). Incidentally, it has been reported by Girimaji and Pope (1990) that the average stretching rate of infinitesimal line (and surface) elements in 3D stationary homogeneous turbulence is also independent of the Reynolds number.

The second test is the DNS of material lines in 2D which are initially Kolmogorov length. In such a case, the extent of a line grows according to the Richardson diffusion, and therefore if

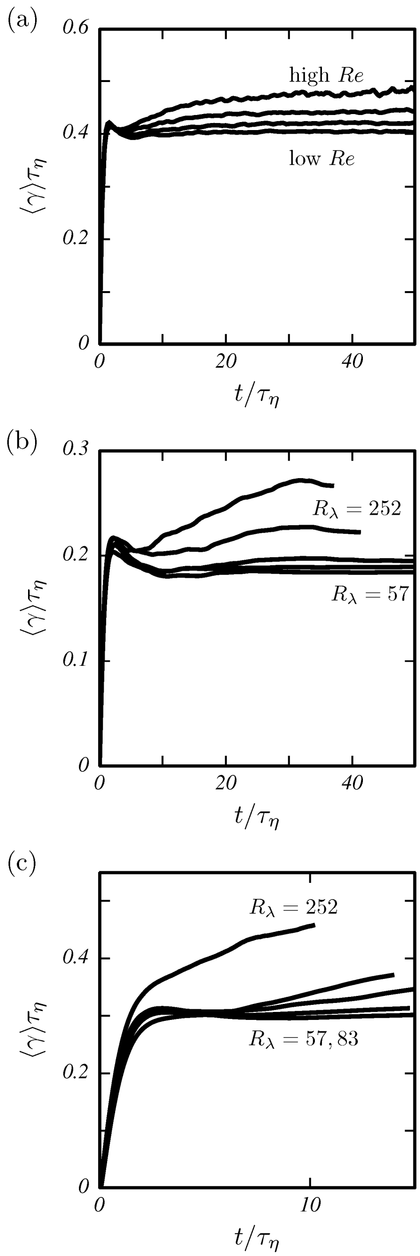

Figure 5: Average stretching rates $\langle\gamma\rangle$, normalised by ${\tau_\eta}^{-1}$, of (a) material lines in 2D, (b) lines in 3D and (c) surfaces in 3D. The initial conditions of the objects are straight lines much longer than $\mathcal{L}$ or flat square surfaces sufficiently wider than $\mathcal{L}^2$. The normalised stretching rates are larger for higher Reynolds numbers.

we normalise the time by the Kolmogorov time, the temporal evolution of the extent is independent of the Reynolds number. Hence, as far as the extent is smaller than the integral scale $\mathcal{L}$ of each flow, the folding of the material lines is statistically similar even if the Reynolds numbers are different. This is because only the eddies smaller than the extent of a line can contribute its folding. Hence, as far as the extent is smaller than $\mathcal{L}$, the average stretching rate is also independent of the Reynolds number. Indeed, this expected behaviour is observed in figure 6(b).

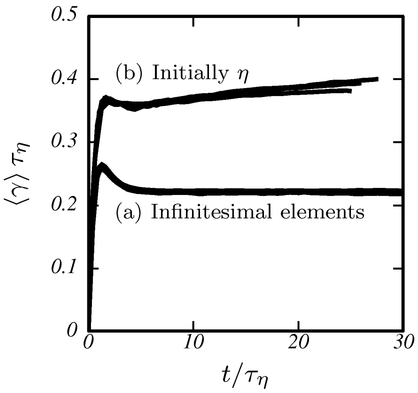

Figure 6: (a) Average stretching rate of infinitesimal line elements in 2D. Four almost identical curves for four different Reynolds numbers are plotted. (b) Average stretching rates of material lines in 2D whose initial length is fixed to be the Kolmogorov length. Four curves for four different Reynolds numbers are plotted.

CONCLUDING REMARKS

In contrast with the conventional idea, the average stretching rate, normalised by ${\tau_\eta}^{-1}$, of sufficiently long material lines (or of wide surfaces) in stationary homogeneous turbulence depends on the Reynolds number; it is larger at higher Reynolds numbers. This does not directly indicate that a singularity, or intermittency, at the smallest scales grows with the Reynolds number, since the average stretching rate of infinitesimal elements does not reveal any Reynolds number dependence. The dependence does not necessarily stem from the two-length-scale property of coherent vortices in 3D turbulence, i.e. sheet- or tube-like structures, since we can see the Reynolds number dependence in 2D as well as in 3D. The physical reason of this Reynolds number dependence may be that the folding of material objects is governed by various-scale eddies while the stretching is dominated by the smallest scale eddies with the time-scale τ_η. The folding by the larger scale eddies lasts longer than τ_η, and the time may become comparable with the integral time $\mathcal{T}$. The combined effect of these small and large time-scales is likely to yield the Reynolds number dependence. Although the two numerical tests have been carried out to confirm this picture, more quantitative argument of the behaviour of stretching rate observed in figure 5 is left for a near-future study.

REFERENCES

Batchelor, G.K., 1952, "The effect of homogeneous turbulence on material lines and surfaces," *Proc. R. Soc. Lond. A* **213**, 349–366.

Girimaji, S. S., and Pope, S. B., 1990, "Material-element deformation in isotropic turbulence," *J. Fluid Mech.* **220**, 427–458.

Goto, S., Kida, S., 2002, "Multiplicative process of material line stretching by turbulence," *J. Turbulence* **3**, 017.

Goto, S., Kida, S., 2003, "Enhanced stretching of material lines by antiparallel vortex pairs in turbulence," *Fluid Dyn. Res.* **33**, 403–431.

Goto, S., Vassilicos, J.C., 2004 "Particle pair diffusion and persistent streamline topology in two-dimensional turbulence," *New J. Phys.* **6**, 65.

Kida, S., Goto, S., 2002, "Line statistics: Stretching rate of passive lines in turbulence," *Phys. Fluids* **14**, 352–361.